Sens. & Instrumen. Food Qual. (2007) 1:62–71
DOI 10.1007/s11694-007-9008-y

ORIGINAL PAPER

Fast line-scan imaging system for broiler carcass inspection

Kuanglin Chao · Chun-Chieh Yang · Yud-Ren Chen · Moon S. Kim · Diane E. Chan

Received: 20 October 2006 / Accepted: 14 February 2007 / Published online: 13 March 2007

Abstract The USDA Agricultural Research Service has developed a fast line-scan imaging system for differentiating wholesome and systemically diseased fresh chickens. The imaging system was used to acquire hyperspectral line-scan images of 250 chicken carcasses on a laboratory processing line moving at 70 birds per minute. A method appropriate for line-scan imaging was developed for automated sensing of birds and locating the Region of Interest (ROI) within the line-scan images most suited for differentiation. From analysis of wholesome and systemically diseased chicken spectra in the ROI, four key wavelengths for differentiating between wholesome and systemically diseased chickens were selected: 424, 465, 515, and 546 nm. The key wavelengths and their ratios with a reference wavelength (689 nm) were investigated for a fuzzy logic based differentiation algorithm. Classification using the key wavelengths correctly identified 98 and 95% of wholesome and systemically diseased chickens for model development, and 98 and 93% of wholesome and systemically diseased chickens for model testing. Although band ratios reduced variation within each chicken category, the resulting classification accuracies were not significantly improved over those for classification by key wavelengths.

Keywords Automated chicken inspection · Food safety · Fuzzy logic · HACCP

K. Chao (✉) · C.-C. Yang · Y.-R. Chen · M. S. Kim · D. E. Chan
Instrumentation and Sensing Laboratory, ARS, USDA, Beltsville, MD 20705-2350, USA
e-mail: chaok@ba.ars.usda.gov

Introduction

Currently, every chicken sold to US consumers is required by law to have been inspected post-mortem by a USDA/FSIS (United States Department of Agriculture/Food Safety and Inspection Service) inspector for its wholesomeness [1]. The inspectors visually examine the exterior, the inner surfaces of the body cavity, and the organs of each carcass for indications of disease or defects. More recently, FSIS implemented the Hazard Analysis and Critical Control Point (HACCP) program in all poultry processing plants throughout the country, and has also been testing the HACCP-based Inspection Models Project (HIMP) at some volunteer plants [2]. This project includes a zero tolerance standard for chickens with septicemia or toxemia, which must be removed from the processing line. For poultry plants to meet government food safety regulations while maintaining their competitiveness to satisfy consumer demand, FSIS has required the development of new inspection technologies [3], such as automated computer imaging inspection systems.

American poultry slaughter plants now process over 8 billion broilers annually. Processing plants seeking to satisfy increasing consumer demand by increasing output through faster processing are limited by the current inspection system, which limits each human inspector to a maximum of 35 birds per minute (bpm). One possible solution to this problem is for poultry processing plants to install online instrumental inspection systems that can accurately screen out unwholesome carcasses. Only questionable carcasses in the rejection line would then require ''re-inspection'' to ensure that wholesome carcasses are not discarded. This approach would dramatically reduce the number of birds requiring human inspection. An obvious benefit of automatic poultry

inspection would be improved overall production efficiency of the processing plants.

The USDA Instrumentation and Sensing Laboratory has developed two automated poultry inspection systems. The first was a visible/near-infrared reflectance spectroscopy system using a fiber optic assembly that acquired a narrow scan across the breast area of chicken carcasses. This system was tested on a 180 bpm commercial processing line and correctly identified 94% of wholesome and 92% of unwholesome birds [4]. The second system was first developed as a dual-camera system using two 20-nm bandwidth interference filters centered at 540 and 700 nm. The system was tested on a 70 bpm commercial evisceration line and achieved 90% classification for separating wholesome and unwholesome chickens [5]. However, the two-camera system was not feasible for high-speed processing lines. Subsequently, a common-aperture camera imaging system was developed using three wavebands at 460, 540, and 700 nm. However, some difficulties were encountered in adjusting the exposure time: an exposure time ideal for the shorter wavelength image was found to result in image saturation at a higher wavelength. During tests on a pilot-scale laboratory processing line, with exposure time adjusted to a compromised value, the system correctly classified 89.6% of wholesome carcasses and 94.4% of systemically diseased carcasses [6]. Most recently, the imaging system was upgraded with an EMCCD camera, which, using an electron multiplying register, allows multiplication of weak signals before readout noise is added by the output amplifier. This system allows more flexibility in adjusting to light conditions, enabling accurate high-speed operation. Changes implemented through the camera control software can allow this line-scan system to operate as a multispectral imaging system. Hyperspectral image data analysis resulted in the selection of key wavelengths for differentiating wholesome and systemically diseased chickens, which can then be implemented for multispectral line-scan operation without the need for cross-system calibration.

The objective of this study was to develop a fast line-scan imaging system for differentiating wholesome and systemically diseased (primarily septiciemic and toxemic) chickens as recognized by FSIS food safety regulations. A method appropriate for line-scan imaging was developed to detect the edge of the bird in the field of view, and the most appropriate Region of Interest (ROI) within each line scan was determined. Spectral differences between wholesome and systemically diseased birds in the ROI area were used to determine key wavelengths for developing a fuzzy logic based algorithm for classification.

Materials and methods

Chicken carcass collection

Eviscerated wholesome and systemically diseased chicken carcasses were identified and collected by USDA FSIS veterinarians at an Allen Family Foods chicken processing plant (Cordova, MD, USA). Chicken carcasses were placed in plastic bags and stored with crushed ice in insulated boxes. The carcasses were then transported, within 2 h, to the Instrumentation and Sensing Laboratory (ISL, USDA-ARS, Beltsville, MD, USA) for the experiments. The carcasses were collected in batches of 10–20 birds over two separate time spans for the following two image sets: 70 wholesome and 76 systemically diseased chickens were collected from August to September of 2005 for the first image set, and 60 wholesome and 44 systemically diseased chickens were collected in October of 2005 for the second image set. Specifically, systemically diseased chicken carcasses collected for this research showed external symptoms of septicemia or toxemia. Septicemia is caused by the presence of pathogenic microorganisms or their toxins in the bloodstream, and toxemia is the result of toxins produced from cells at a localized infection or from the growth of microorganisms.

Hyperspectral line-scan imaging system

The hyperspectral imaging system consisted of an electron-multiplying charge-coupled-device (EMCCD) camera and an imaging spectrograph. The linear field of view is created using a slit in front of the spectrograph. A collimated light beam from each pixel of the scanned line is dispersed to obtain a spectrum, as shown in Fig. 1. For each scanned line, a two-dimensional image of reflectance intensity is created with spatial position along one axis and spectral wavelength along the other. In this system, a PhotonMAX 512b EMCCD camera (Princeton Instruments, Roper

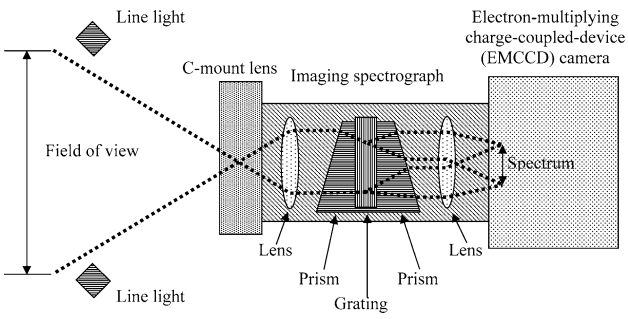

Fig. 1 Diagram of spectral acquisition by the line-scan hyperspectral imaging system for a single pixel, as viewed from overhead

Scientific, Inc., Trenton, NJ, USA), with thermoelectric air cooling down to –70°C to keep the dark current stable, was used to acquire spectral images. The camera operates with a 10 MHz, 16-bit digitizer for low-light, high-speed image acquisition. An ImSpector V10 imaging spectrograph (Spectral Imaging Ltd., Oulu, Finland) was used to produce a contiguous series of spectral images. A Rainbow CCTV S6X11 C-mount lens (International Space Optics, S.A., Irvine, CA, USA) was attached to the spectrograph. This compact lens is manufactured with a broadband coating for wavelengths from 400 to 1,000 nm.

Chicken image acquisition and preprocessing

The hyperspectral line-scan imaging system was used to acquire images of chickens hung on the shackles of a closed-loop pilot-scale processing line moving at 70 birds per minute, reflecting a commonly used operating speed on poultry plant evisceration lines. The field of view was illuminated using a pair of high power, broad-spectrum white light-emitting-diode (LED) line lights (LL6212, Advanced Illumination, Inc., Rochester, VT, USA). The white light from the LEDs is generated by utilizing a blue LED to pump one or more visible light-emitting phosphors integrated into the phosphor-converted LED package. The phosphor then converts most of the blue light into red and green light. The current for the white LED line lights was set at 100 mA. The horizontal distance from the lights to the shackle was 292 mm. The distance between the two lights was 254 mm. Images were acquired with the camera set for a 1 ms exposure time and an absolute multiplication gain of 1.75. A black acrylic background with a matte surface finish was mounted behind the shackles.

The software WinView/32 version 2.5.19.0 (Princeton Instruments, Roper Scientific, Inc., Trenton, NJ, USA) was used to control the hyperspectral imaging system for data acquisition. To increase image acquisition speed, the default line-scan image size, 512×512 pixels, was reduced by binning the pixels by two in the spatial dimension and by four in the spectral dimension, reducing the image size to 256×128 pixels. It was found that, because of natural characteristics of the LED light source and lens, the intensities from the first 19 and the last 6 spectral channels (corresponding to wavelengths below 395 nm and above 1,138 nm) were too low to be used. Discarding these 25 channels, the remaining 103 spectral channels were retained for image acquisition. Thus, the final line-scan image size was 256×103 pixels. To calibrate the relationship between spectral channels and wavelengths, reference peaks from the raw spectra for a mercury–neon pencil light (Oriel Instruments, Stratford, CT, USA) were used. The lamp of the pencil light contains mercury to dominate the output spectrum, and also contains neon as a starter gas. Thus, the output of the pencil light in the first minute of usage is that of neon, and afterwards automatically turns to that of mercury. Then, the following second-order polynomial regression, in which λ is the wavelength in nm and n_c is the spectral channel number, was calculated from the reference wavelength peaks of the mercury and neon spectra, as shown in Fig. 2, to calibrate the spectral axis

$$\lambda = 0.0161 \times n_c^2 + 5.6051 \times n_c + 389.87 \quad (1)$$

The correlation coefficient of the linear regression between calibrated and expected wavelengths was 0.9999. From the wavelength calibration, the image spectrum ranged from 395 nm (the first channel) to 1,138 nm (the 103rd channel) with an average bandwidth of 7 nm. The 140 mm linear field of view was translated into 256 spatial pixels, with each pixel representing an area of 0.55×0.55 mm^2.

The number of line-scan images acquired by the hyperspectral imaging system for each bird varied with the bird size; on average, approximately 130 line-scan images were needed for a wholesome bird and approximately 123 line-scan images for a systemically diseased bird. The line scans were compiled to form complete chicken images, such as the example images shown in Fig. 3. The flat field correction was applied to all chicken line-scan images. The flat field and dark current reference images were collected first each day, and were applied to all line-scan images collected later on the same day. For the flat field image, a Spectralon diffuse reflectance target (Labsphere, Inc., North Sutton, NH, USA) was used as a calibration target. The Spectralon reference target was hung on a shackle and moved through the field of view. The imaging system acquired 20 line-scans of the target, and the average reflectance from these 20 line-scan images was calculated for the flat field reference image W. The lens was covered

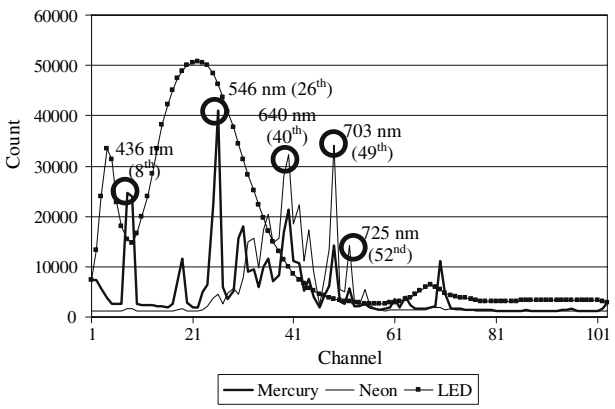

Fig. 2 Spectra for pencil light (Mercury and Neon) and light-emitting-diode (LED) line lights using a Spectralon diffuse reflectance target for wavelength calibration

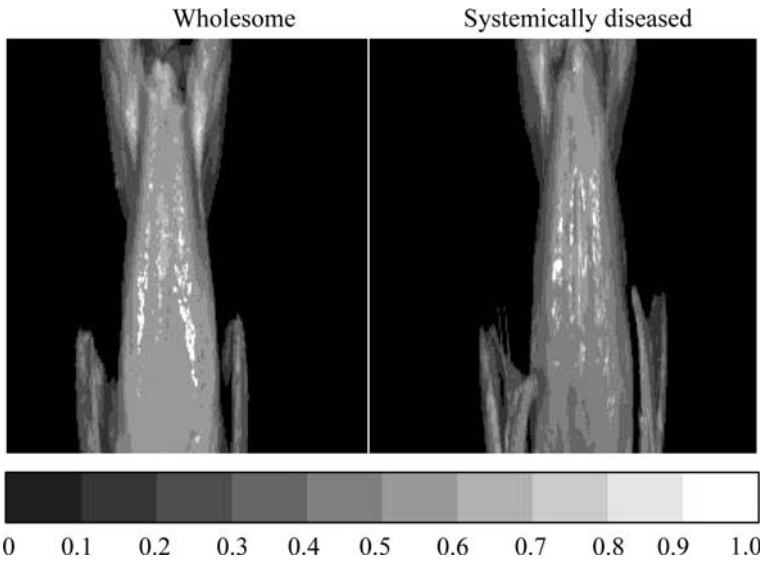

Fig. 3 Compiled reflectance images of a wholesome chicken and a systemically diseased chicken as illuminated by the white LED line lights

completely by an opaque black cloth and the LED line lights were turned off for the acquisition of another 20 line-scan images, and the average reflectance from these images was calculated for the dark current reference image D. For each raw line-scan image I_0, the pixel-based flat field correction was performed to obtain the corrected line-scan image I as follows:

$$I = \frac{I_0 - D}{W - D} \tag{2}$$

The relative reflectance in the corrected line-scan image I was used for image analysis and differentiation. With the use of the black acrylic background during imaging, chicken pixels were easily extracted from darker background pixels by using a relative reflectance threshold value of 0.1 at the 626 nm wavelength, which was selected because the chicken spectra consistently showed the highest reflectance intensities at this wavelength when using the white LED illumination.

Line-scan edge detection, region of interest selection, key wavelength determination

A method appropriate for line-scan imaging was created to detect the entry of each chicken carcass into, and its exit from, the camera field of view. As the camera acquired each new line-scan image, the relative reflectance at 626 nm was examined for each pixel within the uppermost 82.5 mm of the line-scan image, which consisted of 150 pixels in this case. These 150 pixels were termed the Carcass Detection Length as shown in Fig. 4. The initial entry of the carcass into the field of view was recognized when the relative reflectance at 626 nm increased above 0.1 for any single pixel within the carcass detection length. This method only examines the uppermost 150 pixels in order to disregard possible anomalies in the position of the wings or any eviscerated organs when detecting carcass position within the field of view. Once the presence of the bird is recognized, it was necessary to detect the point on the leading edge of the chicken image at the junction of the thigh and the side of the belly, which in Fig. 4 is labeled as the Turning Point. After the first pixel within the carcass detection length was detected with a reflectance greater than 0.1, subsequent scans continued to monitor the pixels in the carcass detection length as additional pixels also began showing relative reflectance values greater than 0.1. As the chicken continued to move across the field of view, pixels below the first detected pixel and above the 150th pixel began increasing in relative reflectance value. As the line-scans continued, the indices of pixels whose reflectance values have not yet turned (greater than 0.1) were noted until, ultimately, a line-scan was found that contains only one pixel (or several adjacent pixels) remaining below the first detected pixel and above the 150th pixel for which the reflectance value is still below 0.1. When the reflectance increased to over 0.1 for that pixel in the next line-scan image, i.e., the reflectance value turned from below 0.1 to above 0.1, then the location of that pixel was identified as the Turning Point. After the identifying the Turning Point, subsequent line-scan images were acquired and the Opposite Turning Point (OTP) was identified when the reflectance value at the pixel location corresponding to the TP turned from above 0.1 to below 0.1, indicating that the main body of the bird had completely passed through the field of view.

Within each line-scan image, beginning with that containing the TP and ending with that containing the OTP, the location of the Region of Interest (ROI) was calculated to fall within the 100% region between the pixel at the TP

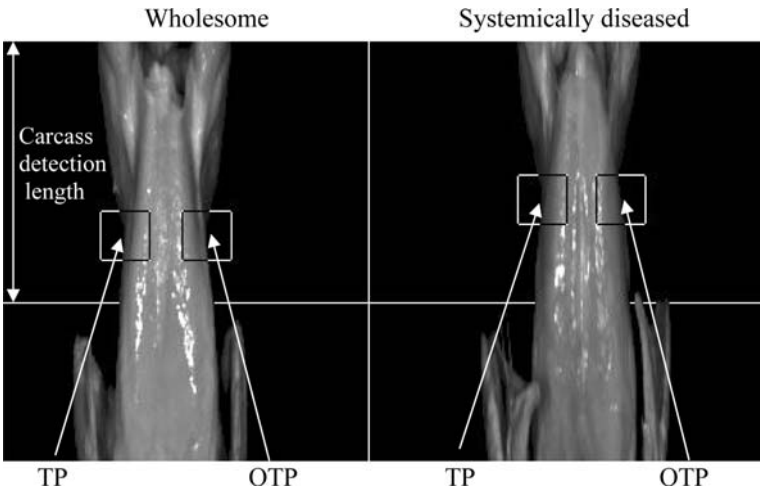

Fig. 4 Carcass detection length, Turning Point (TP), and Opposite Turning Point (OTP)

coordinate and the bottommost non-background pixel of the line-scan image, as shown in Fig. 5. To determine an appropriate ROI to use for classifying wholesome and systemically diseased chickens, 20 combinations of *P* and *Q* were evaluated using values of 10, 20, 30, 40 and 50% for *P*, and values of 60, 70, 80, and 90% for *Q*. ROI pixels were extracted from line-scan images of wholesome birds in the first data set, and the average wholesome spectrum was calculated. Similarly, the average unwholesome spectrum was calculated from ROI pixels extracted from line-scan images of systemically diseased birds in the first data set. A difference spectrum was then calculated between the average wholesome and systemically diseased spectra for each of the 20 ROI. Figure 7 shows the maximum and minimum intensity values that occurred for the difference spectrum of each ROI. The ROI showing the greatest intensity difference between wholesome and systemically diseased chickens was selected as the most appropriate ROI to use for key wavelength determination and differentiation between wholesome and systemically diseased birds.

Fuzzy logic based differentiation algorithm development

The classification algorithm to differentiate between images of wholesome and systemically diseased chickens was based on fuzzy logic. Fuzzy logic is derived from fuzzy set theory, which was introduced by Zadeh [7]. Fuzzy set theory allows for ''imprecise'' set membership values between and including 0 and 1, unlike ordinary set theory which only allows values of 0 and 1. For algorithm development, the Fuzzy Logic Toolbox version 2.1.3 of MATLAB was used (MathWorks, Natick, MA, USA).

To develop the fuzzy logic based differentiation algorithm, a membership function was defined based on individual key wavelengths, using average and standard deviation intensity values. As seen in Fig. 6, each membership function includes two fuzzy sets, one for systemically diseased chicken and one for wholesome chicken. For an input intensity value, the degree of membership in the systemically diseased set was equal to 1 when the intensity input was equal to or less than the

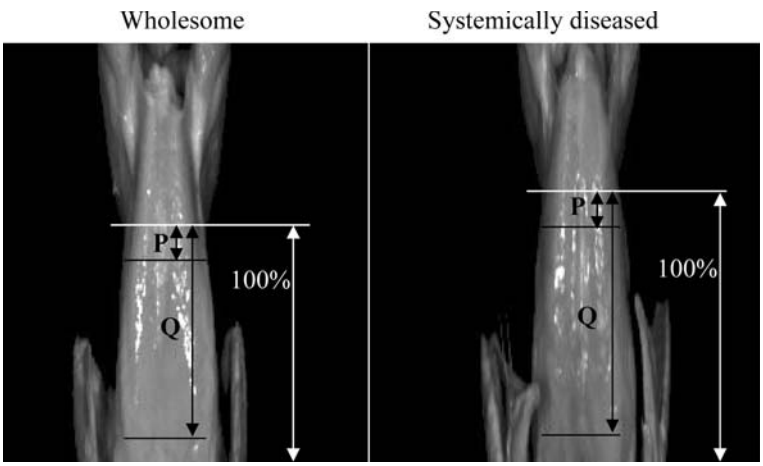

Fig. 5 Locating the region of interest between *P*% and *Q*% of distance from the turning point to the lower chicken edge

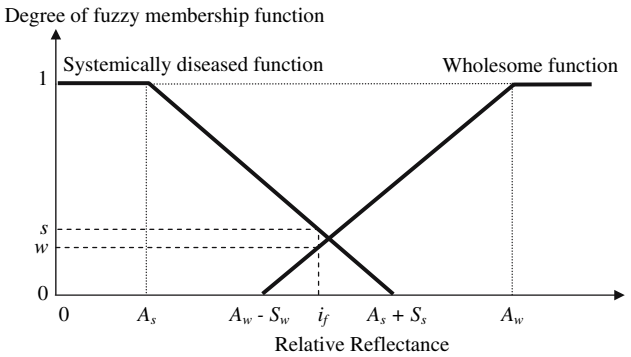

Fig. 6 Construction of fuzzy logic membership function for each key wavelength, for wholesome and systemically diseased chicken, based on reflectance intensity values (mean and one-standard deviation)

average systemically diseased reflectance, A_s. The degree of membership in that set was equal to 0 when the intensity input was equal to or greater than the average intensity value plus one standard deviation, $A_s + S_s$. For input values in between, the degree of membership decreased linearly from 1 to 0. The degree of membership in the wholesome set was based on the values for average intensity, A_w, and average minus one standard deviation, $A_w - S_w$. Here, the degree of membership in the wholesome set was equal to 1 when the intensity input was equal to or greater than A_w. The degree of membership in that set was equal to 0 when the intensity input was equal to or less than $A_w - S_w$. For input values in between, the degree of membership increases linearly 0 to 1.

For each pixel in the line-scan image, a membership function was used with each key wavelength intensity value, i_f, to obtain two corresponding degrees of membership (s and w) in the systemically diseased and wholesome fuzzy sets. The fuzzy inference engine executes a min–max operation [8] to obtain a decision output D_o for each pixel based on the n membership functions as follows:

$$D_o = \max[\min\{w_1 \ldots w_n\}, \min\{s_1 \ldots s_n\}]. \quad (3)$$

The discrete decision output of D_o was 1 when $\min\{s_1 \ldots s_n\}$ was greater than $\min\{w_1 \ldots w_n\}$, indicating the existence of systemic disease; 0 when $\min\{w_1 \ldots w_n\}$ was greater than $\min\{s_1 \ldots s_n\}$, indicating the non-existence of systemic disease (i.e., the evidence of being wholesome); and 0.5 when the two were equal, indicating uncertainty of decision.

The discrete decision output values for all the pixels analyzed were then averaged, and the final decision for the chicken was made using the threshold value of 0.5: for an average value greater than 0.5, the chicken was identified as being systemically diseased; otherwise, the bird was identified as being wholesome. This model was developed using data from the first image set and then independently tested using data from the second image set.

Results

Figure 7 shows the maximum and minimum intensity differences that occurred between wholesome and systemically diseased chickens when considering each potential ROI as defined by P and Q. The ROIs defined more narrowly and more closely around the central breast area showed greater intensity differences than the broader ROIs or those closer to the upper and lower edges. Among all the ROIs, the 50–60% ROI showed the largest maximum and minimum values: 0.205 at 465 nm and 0.173 at 689 nm.

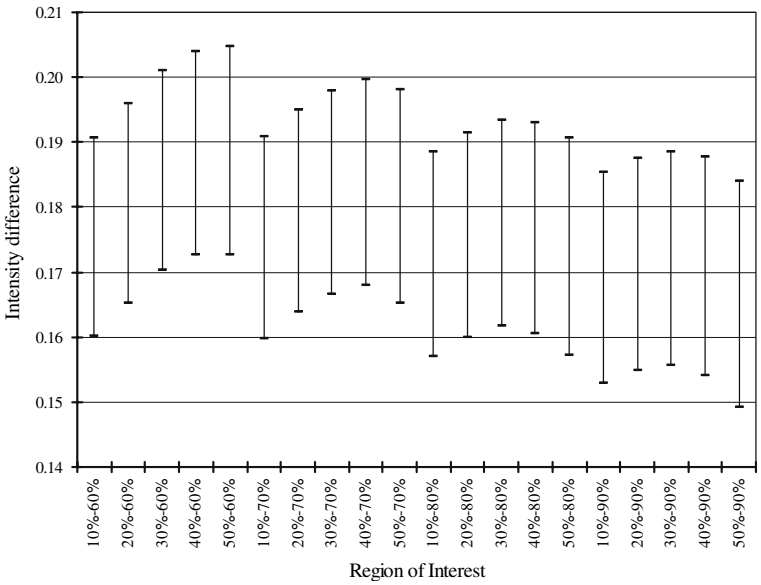

Fig. 7 Maximum and minimum values for intensity difference between wholesome and systemically diseased chickens, for each potential region of interest

This 50–60% ROI was used to determine key wavelengths and to perform further classification of wholesome and systemically diseased chickens.

The 50–60% ROI was used to select pixels from the wholesome chicken images in the first data set, and the average wholesome chicken spectrum over all these pixels was calculated. Similarly, the average systemically diseased chicken spectrum was calculated from the systemically diseased chicken images in the first data set. These spectra are shown in Fig. 8. The spectra for wholesome and systemically diseased chickens were similar in overall shape. The average wholesome chicken spectrum shows higher relative reflectance than the average systemically diseased chicken spectrum across all wavelengths. There is some overlap between the one-standard-deviation envelopes around the average spectra, but the overlap does not include the average spectra; each average spectrum falls outside of 1 standard deviation of the other average spectrum.

From the average wholesome and systemically diseased spectra shown in Fig. 8, the difference spectrum was calculated and is shown in Fig. 9. From the peaks of the difference spectrum, key wavelengths were selected at 424, 465, 515, and 546 nm to develop fuzzy logic based membership functions for differentiation of wholesome and systemically diseased chickens. In addition, a reference wavelength was chosen at 689 nm because the lowest difference between the average wholesome reflectance and average systemically diseased reflectance occurred at this wavelength. Ratios of these four key wavelengths to the reference band were also investigated for developing fuzzy logic based membership functions for differentiation. The ratio of relative reflectance between each key wavelength

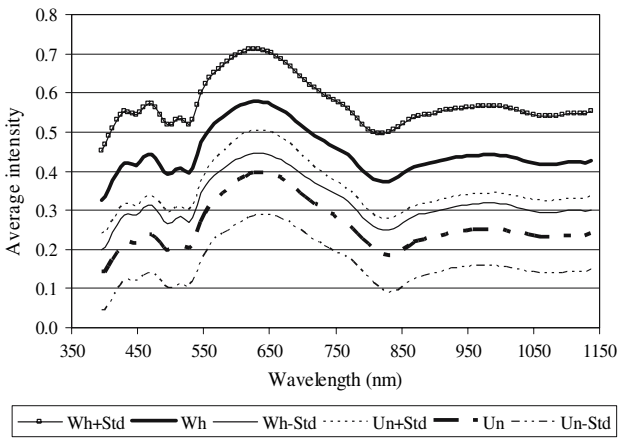

Fig. 8 Average wholesome spectrum and average systemically diseased spectrum, with one standard deviation envelopes, as determined from the region of interest defined by $P = 50\%$ and $Q = 60\%$

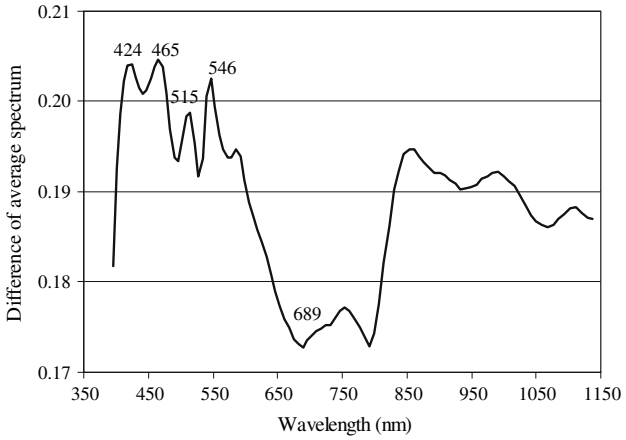

Fig. 9 Difference spectrum calculated from the average wholesome and average systemically diseased spectra for the 50–60% region of interest. Four key wavelengths were selected at 424, 465, 515, and 546 nm and the reference wavelength was selected at 689 nm

I_k and the reference wavelength I_r was calculated as follows:

$$F_{k/r} = \frac{I_k}{I_r}. \quad (3)$$

Membership functions were developed using the four key wavelengths and also four waveband ratios. Using the 50–60% ROI for images of wholesome chickens in the first data set, the average pixel intensity at each key wavelength and the average pixel value for each ratio was calculated. The average pixel intensity at each key wavelength and the average pixel value for each ratio was also calculated using the images of systemically diseased chickens in the first data set. Table 1 shows the average and standard deviation of these values for each key wavelength and each ratio. These values were used to construct two sets of fuzzy logic based membership functions as described in Fig. 6, with one set based on key wavelengths and the other based on ratios, for the classification of chickens.

Using the membership functions based on key wavelengths, the classification results for the first image set show that wholesome and systemically diseased chickens can be easily distinguished from each other, as shown in Fig. 10: 69 of 70 wholesome chickens (98%) and 72 of 76 systemically diseased chickens (95%) were correctly identified. The second image data set was used to validate the fuzzy logic based classification model: 59 of 60 wholesome chickens (98%) and 41 out of 44 systemically diseased chickens (93%) were correctly identified, as shown in Fig. 11.

Using the membership functions based on waveband ratios, the classification model correctly identified 66 of 70 wholesome chickens (94%) and 72 of 76 systemically diseased chickens (95%), as shown in Fig. 12. For the

Table 1 Mean and standard deviation values for the membership functions constructed from relative reflectance intensities at the 424, 465, 515, and 546 nm key wavelengths, and from ratios of the relative reflectance intensities at these key wavelengths

Membership function inputs	Wholesome		Systemically diseased	
	Mean	SD	Mean	SD
I_{424}	0.41	0.13	0.21	0.10
I_{465}	0.44	0.13	0.24	0.10
I_{515}	0.41	0.13	0.21	0.10
I_{546}	0.47	0.13	0.27	0.10
I_{424}/I_{689}	0.77	0.12	0.56	0.18
I_{465}/I_{689}	0.83	0.10	0.65	0.15
I_{515}/I_{689}	0.76	0.10	0.56	0.18
I_{546}/I_{689}	0.89	0.08	0.74	0.13

second image data set, the model correctly classified 57 of 60 wholesome chickens (95%) and 42 out of 44 systemically diseased chickens (95%), as shown in Fig. 13.

Discussion

This fast line-scan imaging system would acquire between 90 and 160 line-scan images for a complete wingtip-to-wingtip image of a chicken carcass. However, such complete imaging is unnecessary for differentiation purposes because the peripheral areas, such as the wings and sides of a bird, may be unpredictably presented during processing conditions and often show irregular shadows impacting reliable reflectance measurements. Most essential is the precise identification of the starting and ending line-scan images for the ROI needed for accurate classification. The method developed in this study to locate the Turning Point and Opposite Turning Point for edge detection of the bird and is ideal for line-scan imaging in the processing environment. Defining the values of P and Q allows the line-scan system to easily locate ROI regardless of bird size occasional and minor shifts in bird position that may occur on the moving processing line. The 50–60% ROI encompassed the image area resulting in the most distinct spectral differences between wholesome and systemically diseased birds in this study, but the ROI can be easily adjusted to adapt to differences that may occur between different populations of chickens in various locations.

Using the membership functions based on waveband ratios achieved classification results that were similar but not improved over classification results from using membership functions based on key wavelengths. The ratios using the 689 nm reference wavelength reduced the variation occurring within each category, as would be expected

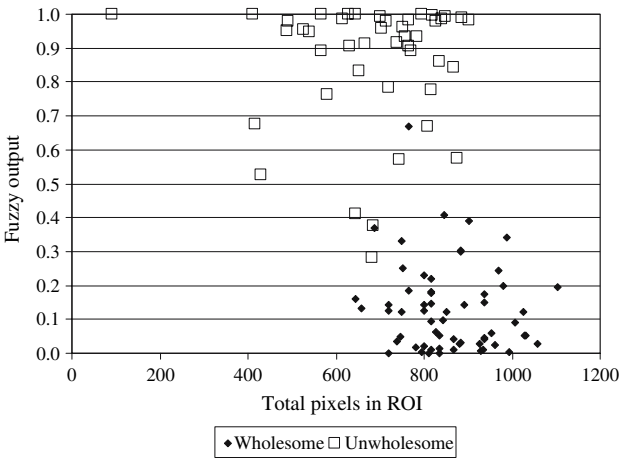

Fig. 11 The fuzzy output for each carcass in the second data set using the key wavelength intensities

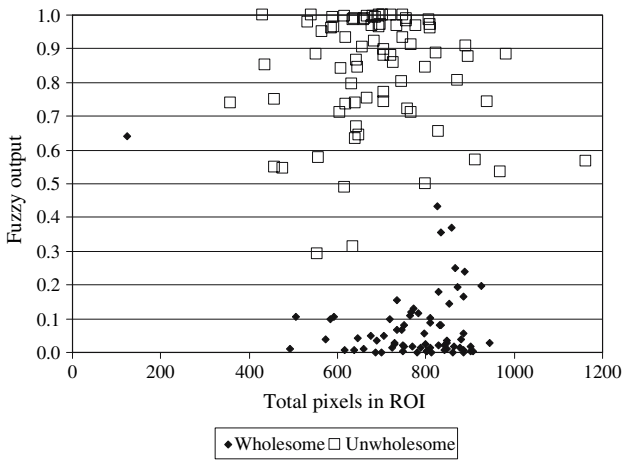

Fig. 10 The fuzzy output for each carcass in the first data set using the key wavelength intensities

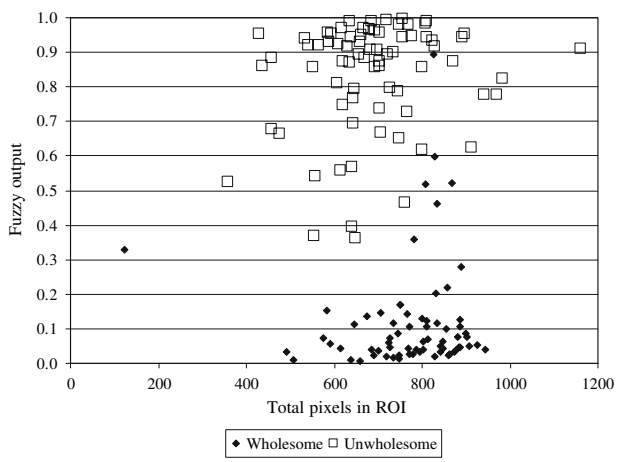

Fig. 12 The fuzzy output for each carcass in the first data set using key wavelength intensity ratios

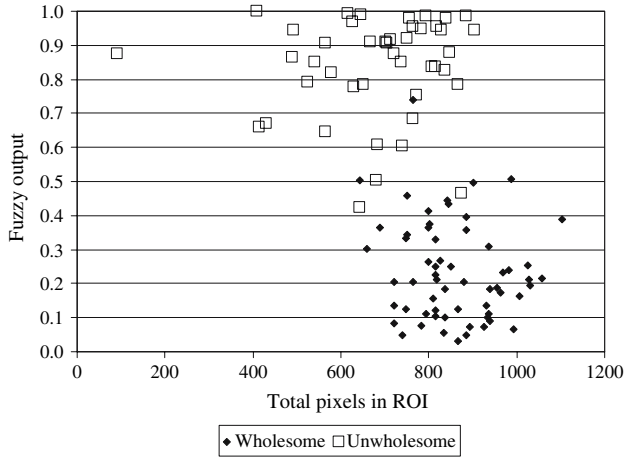

Fig. 13 The fuzzy output for each carcass in the second data set using key wavelength intensity ratios

with the use of band ratios. Within each chicken category (wholesome and systemically diseased), the ratio values showed less variation than the key wavelengths did, with standard deviation values approximately 9–32% of the average values, compared to 30–50% standard deviation values for the key wavelengths, as shown in Table 1. The ratios did not increase the difference between the average wholesome and average systemically diseased chicken values: the average systemically diseased values are approximately 50% of the average wholesome values when using key wavelengths, but range between 73 and 83% when using the ratios. This results from the similarity between the spectra of wholesome and systemically diseased chicken, which primarily show the same reflectance pattern but with vertical shifts in reflectance intensity. Here, the use of band ratios is not as useful as it can be for the identification of dissimilar targets that show more distinct spectra patterns.

The high classification accuracy achieved strongly indicates that the key wavelengths of 424, 465, 515, and 546 nm were appropriately selected for differentiating systemically diseased chickens from wholesome chickens. In particular, the 424 and 546 nm wavelengths were previously found to be closely related to the deoxymyoglobin and oxymyoglobin species associated with chicken meat condition in two-dimensional correlation spectroscopy studies [9, 10].

With key wavelengths determined from the hyperspectral data, the fast line-scan imaging system used in this study can then be reconfigured for high-speed multispectral imaging through camera control settings, without the usual need for cross-system calibration typically required for transferring methods developed from hyperspectral analysis. In this study, hyperspectral images were acquired using 103 channels, but by limiting the system to multispectral operation using only the selected key wavelength channels, imaging speed can be significantly increased. This capacity for rapid operations is crucial to implementing imaging systems for online poultry carcass inspection.

The fuzzy logic based algorithm developed in this study can be applied to other populations of chickens (varying in season, geography, or growth conditions). Inclusion of additional populations will require the collection of additional samples to account for additional variations encountered, resulting in minor modifications to the fuzzy membership functions. This classification method is easily adaptable and simple to implement, and consequently is ideal for line-scan imaging on a high-speed processing line.

By coupling spatial and spectral analysis, this line-scan imaging system can be used for additional food safety inspection for localized disease conditions such as tumors, synovitis, and inflammatory process, as well as food quality concerns such as bruising, overscalding, or broken wings. This is a significant advantage over previously developed spectroscopic systems, which can only measure reflectance from a limited area of each bird. In addition, the line-scan imaging system presents advantages to processing operations by enabling functions such as bird/shackle counting, detection of empty shackles, or statistical measures for quality feedback control, without the installation of proximity sensors or some other devices typically needed for those functions, while remaining comparable in cost to a spectroscopy-only inspection system.

Conclusions

A fast line-scan imaging system was used to acquire images of 250 fresh chickens in two sets: 70 wholesome and 76 systemically diseased chickens for the first image set, and 60 wholesome and 44 systemically diseased for the second image set. The chicken carcasses were hung on a line of shackles moving at a speed of 70 birds per minute for imaging. A method to locate the ROI within each line-scan image was developed and through spectral analysis of the 103 available wavelengths between 395 and 1,138 nm, four wavelengths at 424, 465, 515, and 546 nm were selected as key wavelengths for differentiation. The wavelength of 689 nm was selected as a reference wavelength for calculating band ratios with the key wavelengths. A fuzzy logic based algorithm was developed to differentiate between images of wholesome and systemically diseased chickens. For each scanned line, image features calculated for single pixels were used as inputs to the fuzzy logic algorithm to obtain a discrete decision output, indicating the existence of systemic

disease. Two sets of membership functions were evaluated, one using the four key wavelengths and the second using band ratios of the four key wavelengths. For model development using the key wavelengths, classification accuracies for wholesome and systemically diseased chicken images were 98 and 95%, respectively, and for model testing were 98 and 93%, respectively. For model development using the wavelength ratios, classification accuracies for wholesome and systemically diseased chicken images were 94 and 95%, respectively, and for model testing were 95 and 95%, respectively. The use of ratios decreased variation within each category of chicken condition but did not improve the classification accuracies significantly, as the accuracies from using key wavelengths were already high. Using the four key wavelengths, the fast line-scan imaging system is suitable for online multispectral differentiation of wholesome and systemically diseased chickens on high-speed processing lines.

References

1. USDA *A Review of the Slaughter Regulations under the Poultry Products Inspection Act* (Regulations Office, Policy and Program Planning, FSIS, USDA, Washington, D.C., 1984)
2. USDA *Pathogen Reduction: Hazard Analysis and Critical Control Point (HACCP) Systems*. Final Rule. Fed. Reg. 61: 28805-38855 (USDA, Washington, D.C., 1996)
3. USDA *Standard Operating Procedures for Notification and Protocol Submission of New Technologies* (USDA, Washington, D.C., 2005)
4. K. Chao, Y.R. Chen, D.E. Chan, Appl. Eng. Agric. **20**(5), 683 (2004)
5. K. Chao, Y.R. Chen, W.R. Hruschka, F.B. Gwozdz, J. Food Eng. **51**(3), 185 (2002)
6. C.C. Yang, K. Chao, Y.R. Chen, J. Food Eng. **69**(2), 225 (2005)
7. L.A. Zadeh, Inform. Controls **8**, 338 (1965)
8. K. Chao, Y.R. Chen, H.L. Early, B. Park, Appl. Eng. Agric. **15**(4), 363 (1999)
9. Y. Liu, Y.R. Chen, Appl. Spectrosc. **54**(10), 1458 (2000a)
10. Y. Liu, Y.R. Chen, Y. Ozaki, J. Agric. Food Chem. **48**(3), 901 (2000b)